

Optical Sectioning of Microbial Biofilms

J. R. LAWRENCE,^{1*} D. R. KORBER,² B. D. HOYLE,³ J. W. COSTERTON,³ AND D. E. CALDWELL²

National Hydrology Research Institute, Environment Canada, 11 Innovation Boulevard, Saskatoon, Saskatchewan, Canada S7N 3H5¹; Department of Applied Microbiology and Food Science, University of Saskatchewan, Saskatoon, Saskatchewan, Canada S7N 0W0²; and Department of Biological Sciences, University of Calgary, Calgary, Alberta, Canada T2N 1N4³

Received 24 May 1991/Accepted 9 August 1991

Scanning confocal laser microscopy (SCLM) was used to visualize fully hydrated microbial biofilms. The improved rejection of out-of-focus haze and the increased resolution of SCLM made it preferable to conventional phase microscopy for the analysis of living biofilms. The extent of image improvement was dependent on the characteristics of individual biofilms and was most apparent when films were dispersed in three dimensions, when they were thick, and when they contained a high number of cells. SCLM optical sections were amenable to quantitative computer-enhanced microscopy analyses, with minimal interference originating from overlying or underlying cell material. By using SCLM in conjunction with viable negative fluorescence staining techniques, horizontal (*xy*) and sagittal (*xz*) sections of intact biofilms of *Pseudomonas aeruginosa*, *Pseudomonas fluorescens*, and *Vibrio parahaemolyticus* were obtained. These optical sections were then analyzed by image-processing techniques to assess the distribution of cellular and noncellular areas within the biofilm matrices. The *Pseudomonas* biofilms were most cell dense at their attachment surfaces and became increasingly diffuse near their outer regions, whereas the *Vibrio* biofilms exhibited the opposite trend. Biofilms consisting of different species exhibited distinctive arrangements of the major biofilm structural components (cellular and extracellular materials and space). In general, biofilms were found to be highly hydrated, open structures composed of 73 to 98% extracellular materials and space. The use of *xz* sectioning revealed more detail of biofilm structure, including the presence of large void spaces within the *Vibrio* biofilms. In addition, three-dimensional reconstructions of biofilms were constructed and were displayed as stereo pairs. Application of the concepts of architectural analysis to mixed- or pure-species biofilms will allow detailed examination of the relationships among biofilm structure, adaptation, and response to stress.

Biofilms are organized multicellular systems with structural and functional architecture which influence metabolic processes, response to nutrients, resistance to antimicrobial agents, predation, and other factors. Structural studies of microbial biofilms and their formation have been performed by using light microscopy to examine wet mounts (16, 23), by using transmission and scanning electron microscopy (12-15, 24), and by developing conceptual models (12). Electron microscopy techniques are laborious and can produce artifacts resulting from sample preparation and limit three-dimensional (3D) reconstruction of biofilms. Light microscopy used in conjunction with computer-enhanced microscopy (CEM) is an effective tool, but it is best applied during the early phases of biofilm development (7, 16, 19, 20). Scanning confocal laser microscopy (SCLM) offers the promise of detailed visualization of thick microbiological samples in cases in which application of traditional phase or fluorescence microscopy is limited. SCLM allows elimination of out-of-focus haze, and it allows horizontal and vertical optical sectioning (0.2- μm intervals), determination of 3D relationships of cells, and 3D computer reconstruction from optical thin sections. In addition, images can be quantitatively analyzed by using image-processing techniques (5, 20). Extensive reviews of the application of SCLM to biological materials have recently been published (1, 4, 9, 10, 25-27). However, applications in microbiology have been limited. The objective of this study was to utilize SCLM and CEM techniques to analyze the biofilm architecture of

several bacterial species grown in continuous-flow slide cultures.

MATERIALS AND METHODS

Bacterial strains and culture conditions. *Pseudomonas fluorescens* CC-840406-E, *Pseudomonas aeruginosa* 579, and *Vibrio parahaemolyticus* BB22 (translucent variant) were routinely cultivated in 10% Trypticase soy broth (3 g · liter⁻¹) (Difco Media Co.), minimal growth medium [$\text{Na}_2\text{HPO}_4 \cdot 7\text{H}_2\text{O}$ (3 mM), KH_2PO_4 (2 mM), $(\text{NH}_4)_2\text{SO}_4$ (0.8 mM), $\text{MgSO}_4 \cdot 7\text{H}_2\text{O}$ (0.4 mM), $\text{Ca}(\text{NO}_3)_2 \cdot 4\text{H}_2\text{O}$ (0.02 mM), glucose (0.1% wt/vol), $\text{FeSO}_4 \cdot 7\text{H}_2\text{O}$ (0.9 μM)], and 75% 2216 marine broth (28 g · liter⁻¹) (Difco marine broth; Difco Media Co.), respectively. *V. parahaemolyticus* BB22 was obtained from M. Silverman (Agouron Institute, La Jolla, Calif.) and was shown to inducibly produce lateral flagella in response to surface contact (3). All pure cultures were stored on glass beads at -80°C. Biofilms were prepared by inoculating continuous-flow slide culture chambers with a suspension of log-phase cells obtained from batch cultures grown in 50 ml of the appropriate medium on a gyrator shaker at 23 \pm 2°C. Construction, preparation, and inoculation of slide culture chambers have been described previously (7, 8, 16). Chambers were irrigated with the appropriate sterile medium at a bulk flow rate of 10 cm s⁻¹ (8 μm s⁻¹ in the surface microenvironment) (17, 19) by using a peristaltic pump (Watson Marlow 201Z). Flow was maintained for 24 to 48 h at 23 \pm 2°C before biofilms were viewed with either SCLM or phase microscopy.

Laser microscopy. Images were obtained with an MRC-500

* Corresponding author.

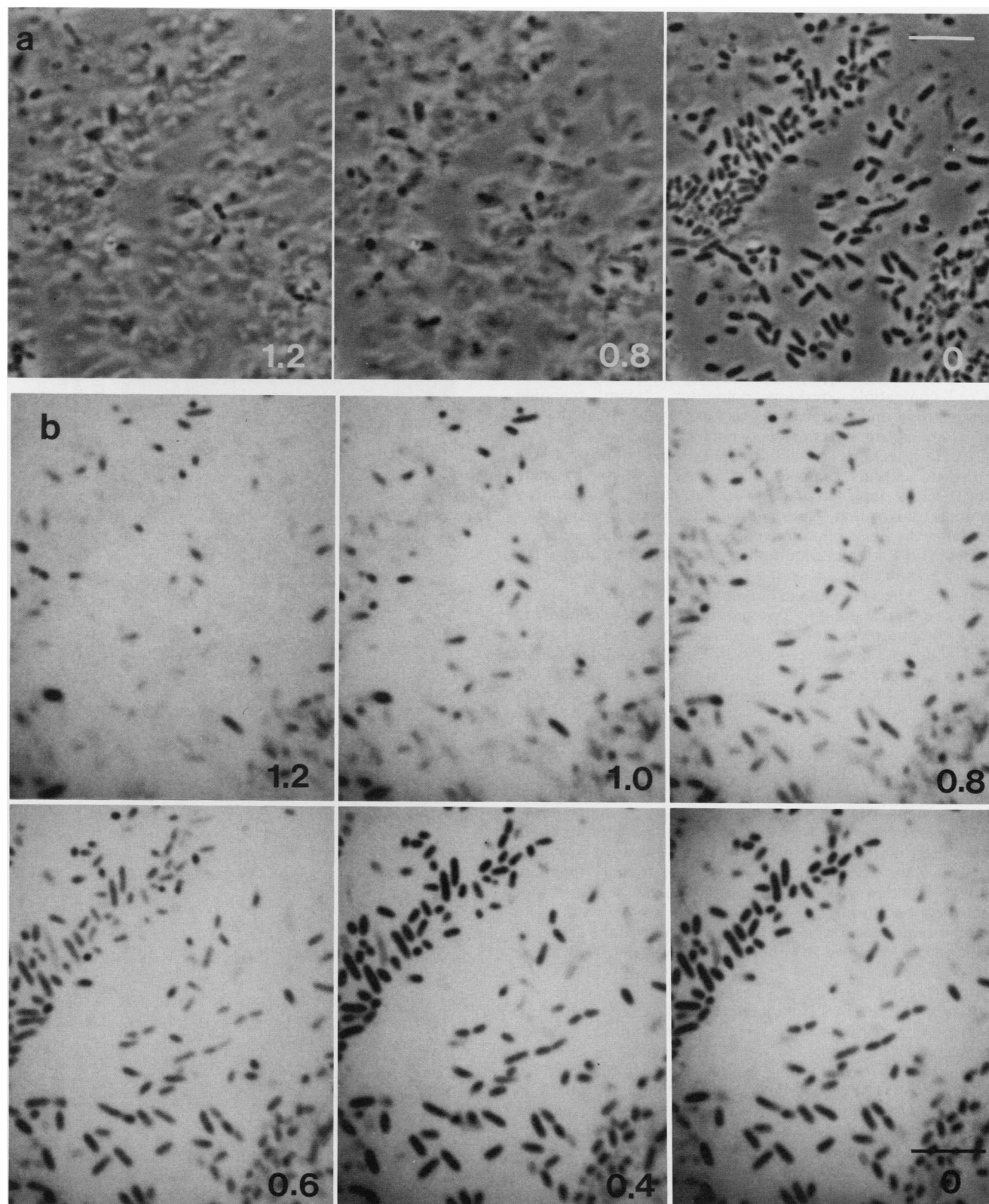


FIG. 1. (a) Conventional phase-contrast photomicrographs of a 48-h *P. fluorescens* biofilm indicating approximate levels of the focal plane in micrometers. Images are arranged in descending order from the outer surface of the biofilm (1.2 μm) to the glass (0 μm). Bar = 5 μm . (b) SCLM images showing a series of horizontal optical sections of the 48-h *P. fluorescens* biofilm shown in panel a. The sections were taken at 0.2- μm intervals (glass surface = 0 μm) with negative fluorescence staining (0.1% fluorescein). Bar = 5 μm .

Lasersharp fluorescence scanning confocal microscope (Bio-Rad Microscience, Toronto, Ontario, Canada) in conjunction with a Zeiss Photomicroscope III (Zeiss, Oberkochen, Germany). The photomicroscope was equipped with a 100 \times , 1.3-numerical aperture (NA) oil immersion, phase-contrast lens. Optical theory predicts that high-NA lenses have the ability to reduce the thickness of the focal region (25). When used in conjunction with confocal laser technology, high-NA lenses have the potential to produce images with sub-200-nm horizontal resolution in the xy axis and with reduced defocused information from xz materials. Phase-contrast microscopy was conducted with a 100-W tungsten lamp (Zeiss Illuminator 100), a green interference filter (Zeiss VG-9; 46-78-05; 546 ± 10 nm), and a 100 \times , 1.3-NA oil immersion lens. An argon laser with maximum emission lines at 488 and 514 nm was used as the excitation source for the fluorophores. The fluorophore fluorescein was injected into the flow cells at a concentration of 0.1%, allowing bacterial cells to be visualized by fluorescence exclusion (6). The scanning control and the image processor were housed in an IBM PC/AT-compatible desktop computer. Beam scanning through the x and y directions was facilitated through the use of galvanometrically controlled mirrors. Intervals between optical thin sections (xy section separation) and the positions of sagittal sections (xz position) were user definable by using the Bio-Rad interactive software in conjunction with a computer-controlled, motor-driven focusing system connected to the Zeiss photomicroscope. Images were collected with a Bio-Rad photomultiplier pickup device and were integrated and digitized with a Kalman true-running-average filter (25). The video image obtained (512 by 512 pixels) was displayed on a standard color monitor. Black-and-white and color computer monitors were photographed with a Kodak CRT cone and an Olympus OM-2n camera equipped with a 49-mm telemacro lens. Photographs were taken with either Plus-X 125 ASA or Ektachrome 200 ASA film (Kodak, Rochester, N.Y.).

Optical thin sections for the construction of stereoscopic images of *V. parahaemolyticus* biofilm material were obtained with the Zeiss LSM 100/Axiophot microscope combination equipped with a 63 \times , 1.4-NA oil immersion, phase-contrast lens. Initially, seven images were collected at 2.0- μ m intervals. These images were then serially arranged and stereo pairs were created with the software provided with the Zeiss laser microscope system. An image intensity control function was used to normalize the brightness of each section during the calculation of stereo pairs. The reconstruction used was one which exaggerated the apparent xz depth for maximal 3D effect, and it was not used for xz distance measurements.

Image analysis. Image processing and analyses were performed with an IBAS 2000 image analysis computer (Kontron, Eching, Germany). Images on photographic negatives were converted to a video signal with a light table illuminated by 4- to 75-W flood lights (color temperature of 2,820 K). An RCA (Lancaster, Pa.) TC1005 plumbicon tube television camera equipped with a 49-mm telemacro lens was used to convert illuminated negatives into an analog video signal (20). The analog video signal was then digitized (768 by 512 by 8 bits) by using image averaging to eliminate random electronic noise originating within the system. Digitized images were then discriminated (20) to differentiate cellular from noncellular material in the biofilm. The cell boundaries were defined, and the number of cells, the cell area, and the percentage of cell area were measured as described previously (7).

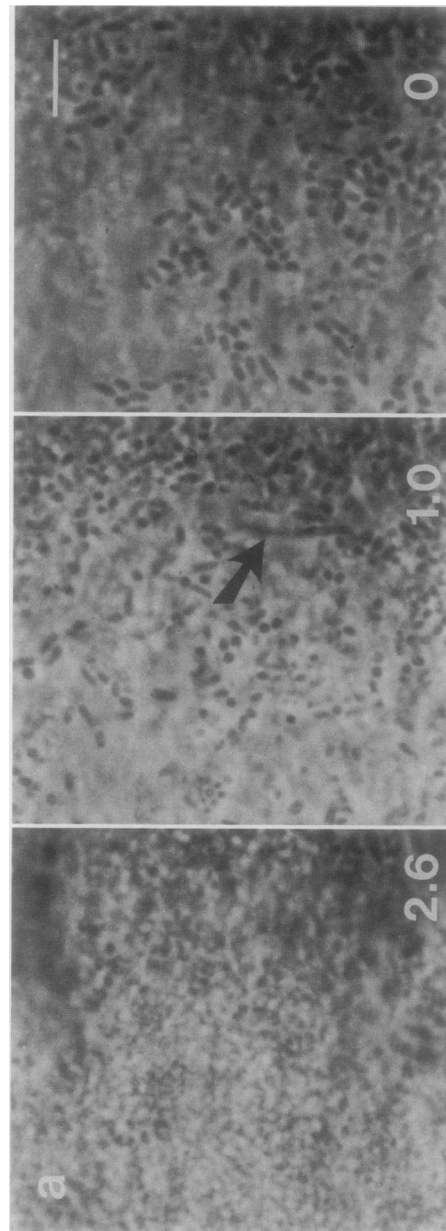


FIG. 2. (a) Phase-contrast photomicrographs of a 48-h *V. parahaemolyticus* biofilm (0 to 2.6 μ m). The middle focal plane (1.0 μ m) shows an elongated cell (arrow) which is evident in several optical sections with SCLM as shown in panel b. Bar = 5 μ m. (b) SCLM images of the *V. parahaemolyticus* biofilm showing the form and arrangement of cells within the biofilm. An elongated *Vibrio* cell (arrow) appears in two optical thin sections (0.8 and 1.0 μ m) but is clearly not seen in other sections. In addition, the biofilm appears to contain fewer cells as the glass surface (0 μ m) is approached. Bar = 5 μ m.

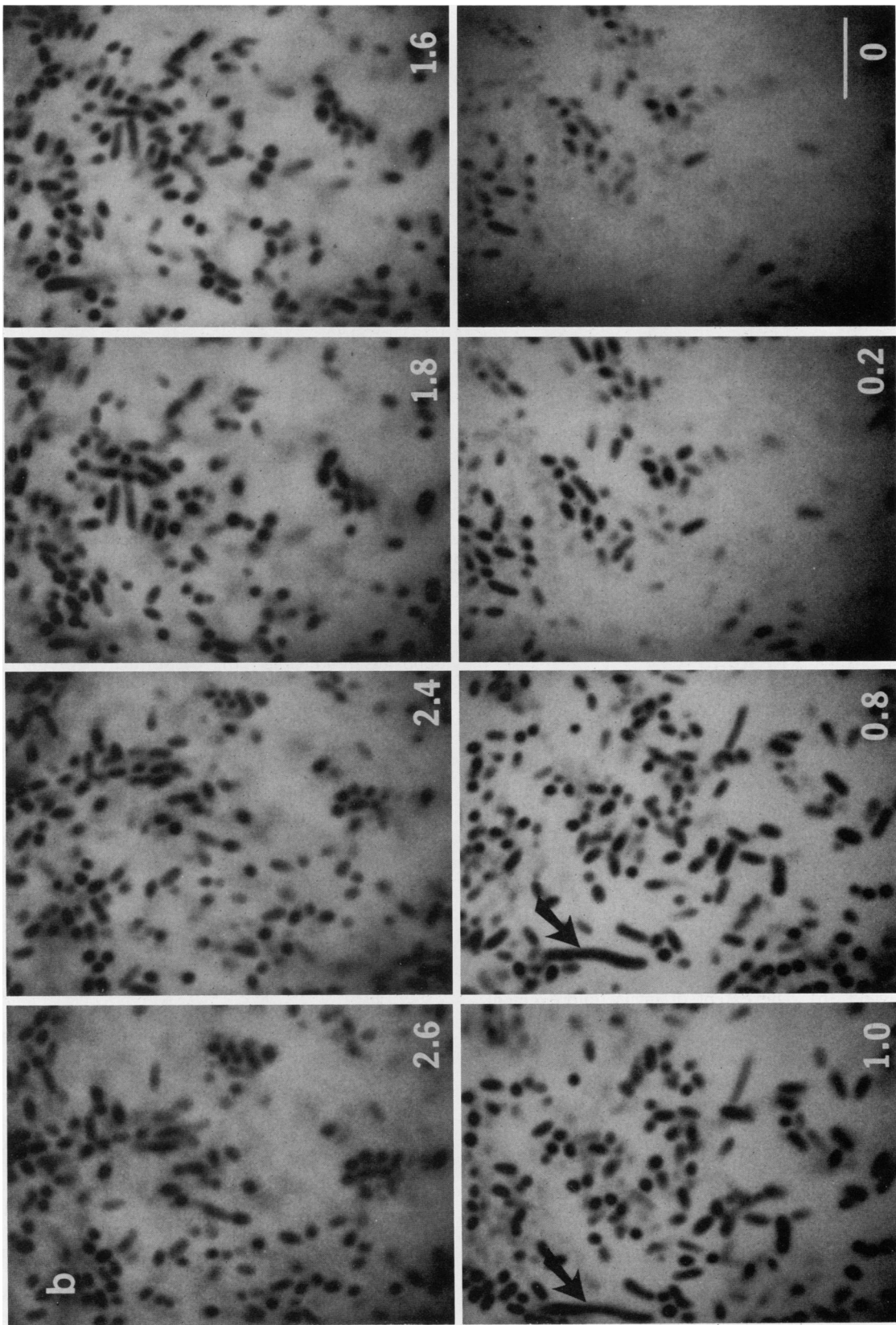


FIG. 2—Continued.

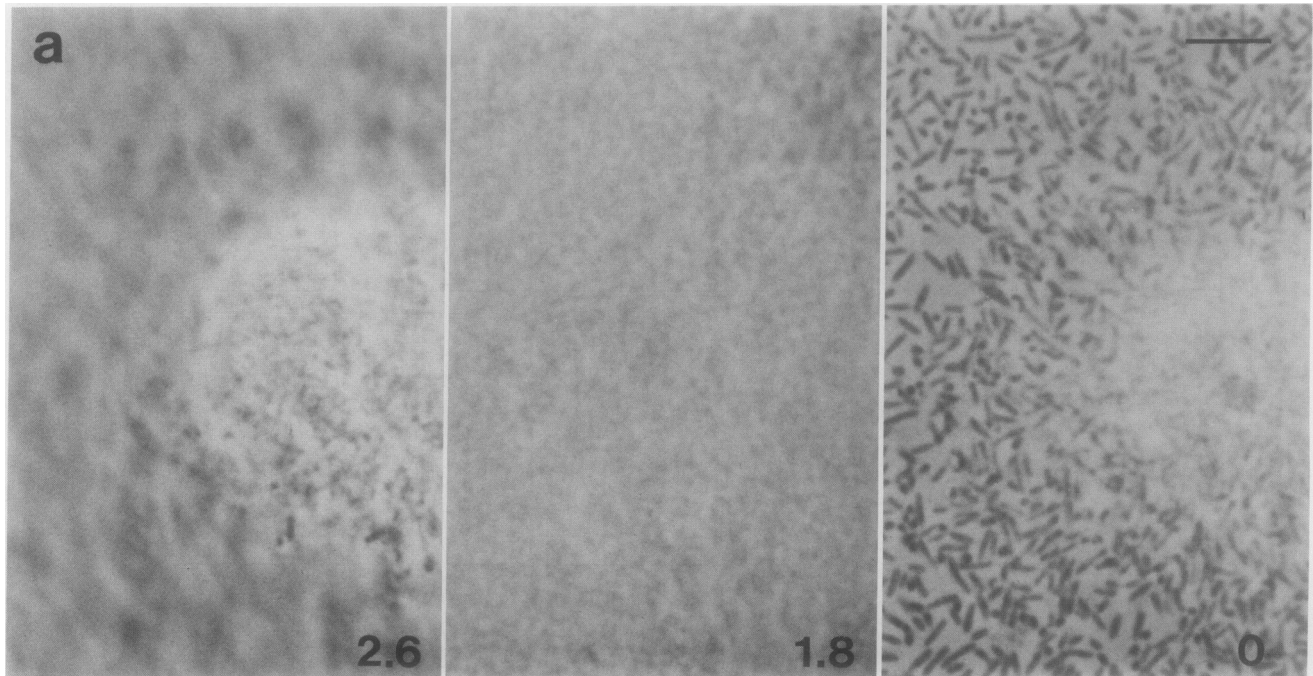


FIG. 3. (a) Conventional phase-contrast photomicrographs of *P. aeruginosa* biofilm showing the surface focal plane (0 μm) and the increase in defocused information at focal planes away from the glass surface. Bar = 5 μm . (b) Horizontal optical thin sections (0 to 2.6 μm) of the *P. aeruginosa* biofilm shown in panel a and obtained by SCLM. The biofilm was negatively stained with 0.1% fluorescein. The horizontal sections show the removal of out-of-focus information and reveal aspects of the internal structure of the biofilm. Bar = 5 μm .

RESULTS

Comparison of phase and SCLM images. SCLM allowed in-focus images to be obtained regardless of the position of the optical section within the biofilm. Phase studies of the *P. fluorescens* biofilm (Fig. 1a) provide reasonable images of the cells located at the glass surface; however, the 0.8- and 1.2- μm sections contain blurred information originating from overlying and underlying cell material. The *V. parahaemolyticus* (Fig. 2a) and *P. aeruginosa* (Fig. 3a) biofilms were more than twice as thick ($\sim 2.6 \mu\text{m}$) as the *P. fluorescens* biofilm; therefore, phase section images were seen to deteriorate in quality and in the information contained. In contrast, SCLM optical sections (0.2- μm increments) were amenable to quantitative CEM analyses, with minimal interference originating from overlying or underlying cell material (Fig. 1b, 2b, and 3b). The extent of image improvement depended upon the characteristics of individual biofilms and was most apparent when films were dispersed in three dimensions, when the biofilm was thick, and when high densities of cells were present. Conventional phase techniques provided images with excessive out-of-focus information from other sections, making measurements of all but general biofilm parameters impossible.

Horizontal optical thin sectioning of bacterial biofilms. Horizontal sectioning showed the form and arrangement of cells of *P. fluorescens*, *P. aeruginosa*, and *V. parahaemolyticus*, and it indicated complete penetration of the biofilms by the 289-molecular-weight fluorescein molecules in less than 1 min. All biofilms exhibited variation with depth in the ratio of cellular to noncellular material. The *Pseudomonas* biofilms were more tightly packed at their attachment surfaces and became increasingly diffuse near their outer regions (Fig. 3b), whereas the *Vibrio* biofilms exhibited the

opposite trend (Fig. 2b). CEM analyses confirmed this distribution of cells (Fig. 4) and showed that the biofilms were highly hydrated, open structures composed of 73 to 98% noncellular material (including exopolysaccharides [EPS] and pore space). The *P. aeruginosa* biofilm had a higher cell-to-noncellular-material ratio, having 9 to 27% cellular material in each optical section (with the highest cell density [27%] occurring at the surface). In contrast, *P. fluorescens* biofilms showed a similar cell arrangement overall, but a much lower cell-to-noncellular-material ratio (2 to 11.5%) was observed in each optical section. The *V. parahaemolyticus* biofilm was characterized by a markedly different cell arrangement, with the biofilm appearing as an inverted pyramid of cells. CEM analyses revealed that the lowest cell density (4%) was at the glass surface and that the highest cell density (13 to 16%) was near the outer region of the biofilm (Fig. 2b and 4).

Sagittal sectioning of bacterial biofilms. SCLM also allowed sagittal (xz) sectioning of biofilms (i.e., vertical thin sections cut through the biofilm from the glass to the exterior surface). Figures 5a through c show a series of sagittal sections through a portion of a *Vibrio* biofilm, revealing the presence of extensive void spaces within the inner regions of the biofilm, and they also illustrate the resolving power of SCLM. The extended section through the biofilm (Fig. 5d) shows the inverse nature of the cell distribution as described on the basis of horizontal sections and CEM analyses. The orientation of the cells in the basal layer of the biofilm is also evident in these laser micrographs.

Stereoscopic images (3D) from optical thin sections. Figure 6 shows a 3D reconstruction of a 14- μm -thick *V. parahaemolyticus* biofilm resulting from the compilation of seven individual thin sections. The reconstruction is presented in

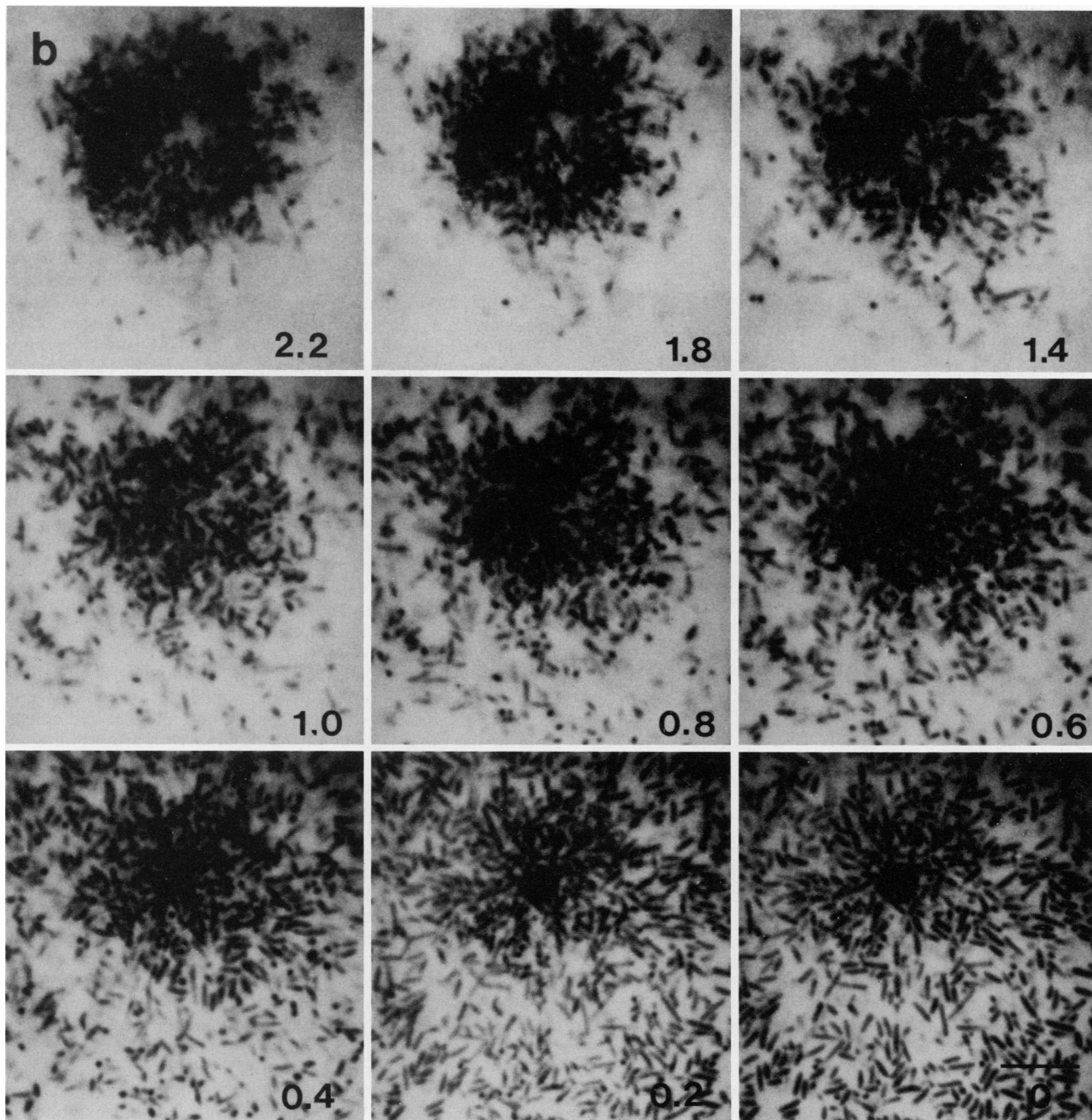


FIG. 3—Continued.

the form of a stereo pair. The presence of extensive void spaces and the relative horizontal distances between cells in the biofilm are easily visualized in this form of data display. However, the vertical distances in the reconstruction are a function of the projection chosen and do not represent the true distances between sections.

DISCUSSION

The results described in this paper demonstrate the potential for noninvasive imaging of intact biofilms and confirm

the effective increase in resolution and depth of field and the elimination of out-of-focus information through the application of SCLM to biofilm studies. Furthermore, the reduction of haze in the SCLM images results in output amenable to computer image analysis. Cell boundaries obtained from SCLM sections are easily discriminated, allowing the determination of cell number and cell area and the estimation of cellular biomass. A major advantage of light microscopy is its ability to allow examination of fully hydrated living biological specimens. This advantage is fully maintained with SCLM. For example, SCLM used in conjunction with

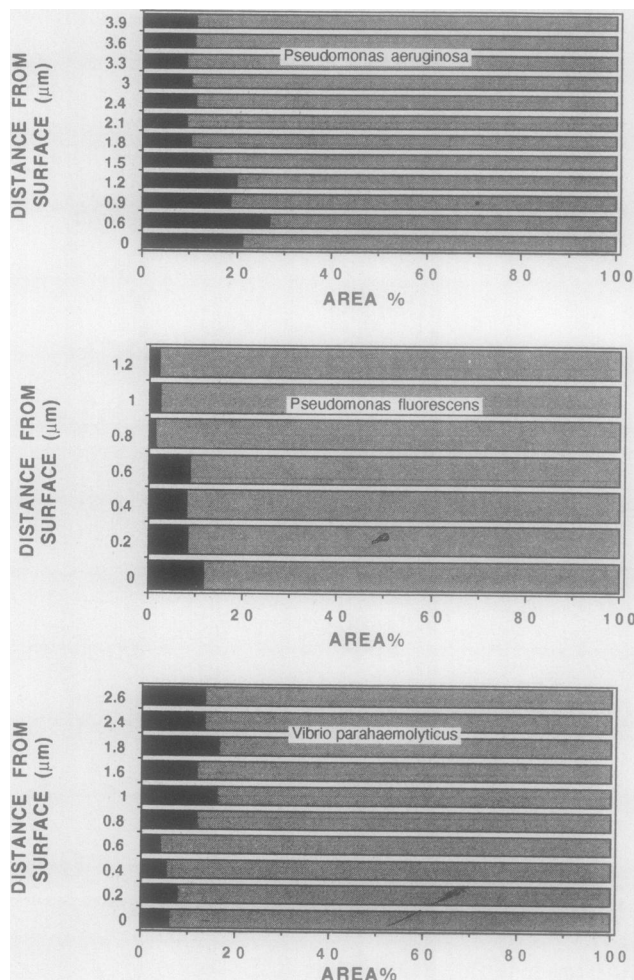


FIG. 4. Quantitative CEM analysis of horizontal sections of *P. fluorescens*, *V. parahaemolyticus*, and *P. aeruginosa*. CEM analysis indicated that all three biofilms were highly hydrated structures composed of 80 to 95% noncellular material. The *Pseudomonas* biofilms were characterized by a dense cell mass in the basal region (glass surface = 0 μm) with increased amounts of extracellular material at the biofilm-liquid interface. In contrast, the *V. parahaemolyticus* biofilm appeared as an inverted pyramid of cells with most noncellular material found at the biofilm-glass interface. ■, percent cellular material; □, percent noncellular material.

fluorescence exclusion techniques (6) has been shown to allow time courses of bacterial microcolony development to be recorded. In contrast, biofilm preparation for electron microscopy may induce morphological changes (dehydration, embedding, and disruption), leading to shrinkages of 50% during fixation (28). Also, time course analysis of biofilm development by electron microscopy would prove difficult. Therefore, the combination of digital image processing and confocal laser microscopy makes optical sectioning of microbial biofilms a practical procedure. The high-resolution capability (200 nm) is apparent in the comparison of phase-contrast and SCLM xy images shown in the figures. Individual cells situated in each SCLM scan plane are clearly visible, without any defocused interference from overlying or underlying cell or noncellular materials.

Architectural analysis of biofilms has been essentially impractical (because of treatment-induced structural

changes) in the absence of SCLM techniques. Morphologically, a biofilm is an open system of cells, exopolymeric material, and extracellular spaces. The spatial arrangement of the cells, EPS, and space may be referred to as the biofilm's architecture. The objectives of architectural analysis are to identify the significant components of biofilm structure and to facilitate quantitative analysis and investigation. SCLM allows this type of approach and should provide for quantitative analyses of structure and of the influence of environmental and induced factors. Costerton (11) has discussed structure and plasticity at different levels of organization in the bacterial cell, including biofilm development as a consequence of attachment to surfaces. The architectural arrangement of a biofilm could be a chance occurrence, but it may represent an optimal arrangement for influx of nutrients, transfer of wastes, and establishment of microenvironmental conditions, etc., subject to change as the biofilm progresses from initial to more established stages. For example, during the initial stages of biofilm formation, distinct microcolony formation and behavior have been observed (16, 18, 19). In the present SCLM study, mature biofilms observed showed no evidence of distinct microcolonies, indicating redistribution of cells within the biofilm during development.

The examination of optical sections through the biofilms revealed significant species-specific architecture. *P. fluorescens* and *P. aeruginosa* followed the expected trends with respect to cell density versus position within the biofilm. The highest concentrations of cells within *Pseudomonas* biofilms were observed closest to the solid-liquid interface (Fig. 1b and 3b). In these cases, the basal biofilm layer provided the foundation for a more diffuse upper layer of cells. In contrast, *V. parahaemolyticus* maintained a higher cell density near the outer regions of the biofilm, with a more disseminated foundation of underlying cells (Fig. 2b). In addition, significant channeling and porosity of the biofilm were observed. This fundamental difference in biofilm structure may be attributed to the role of lateral flagella (2) in the attachment of *Vibrio* cells during surface colonization and biofilm development, as well as the apparent reduced significance of EPS in *Vibrio* biofilms.

The ratio of cellular to noncellular material varied considerably among species and also between optical sections (Fig. 4). The highest ratios were observed for *P. aeruginosa* biofilms. In addition, a central zone within the *P. aeruginosa* biofilm showed increased cell density in association with surface detritus. A similar phenomenon was noticed in tap-water biofilms by Kellogg (14). The *P. fluorescens* biofilms contained less cell material at all optical sections than did those of *P. aeruginosa* and were less developed vertically. In contrast, *V. parahaemolyticus* biofilms exhibited an inverted structure. Maintenance of a minimal basal layer is likely important in preventing uncontrolled sloughing of the biofilm, or this depopulation of the basal layer may precede sloughing. The tortuous nature of biofilms has previously been reported or hypothesized following a number of different studies, the majority of them relying on scanning electron microscopy and transmission electron microscopy observation of fixed biofilm specimens. Robinson et al. (24) reported that studies of biofilms from anaerobic fixed-bed reactor surfaces revealed an extensive network of channels throughout the film matrix, and the researchers indicated that these ultrastructural formations could function to maintain gas and nutrient exchange within the basal layer of the biofilm. Our findings with *V. parahaemolyticus* (a facultative anaerobe) revealed similar biofilm architecture that also

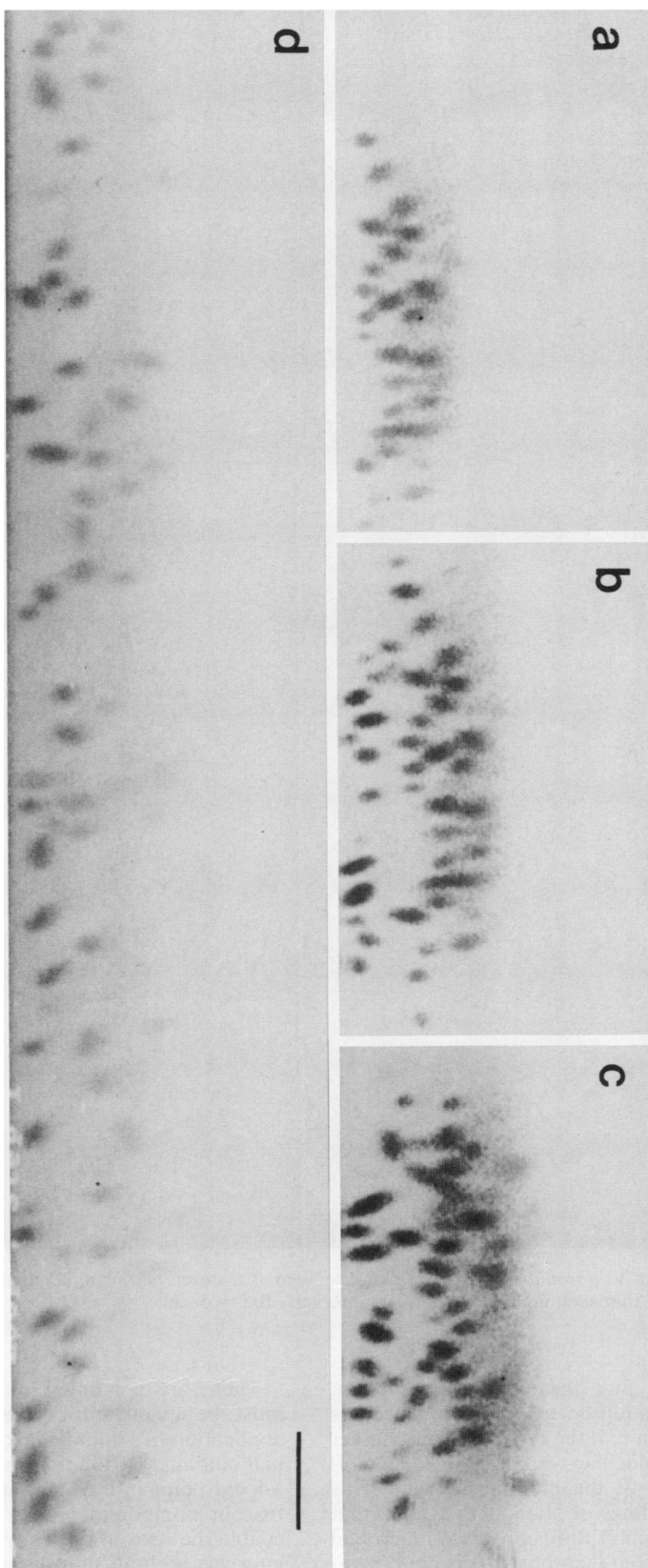


FIG. 5. Series of sagittal sections (xz optical thin section) at various positions through a *Vibrio* biofilm, showing the form and arrangement of cells in vertical cross section. These views show the hydrated open nature of the *V. parahaemolyticus* biofilm and the relationship of cells to one another and to the substratum. Bar = 5 μ m.

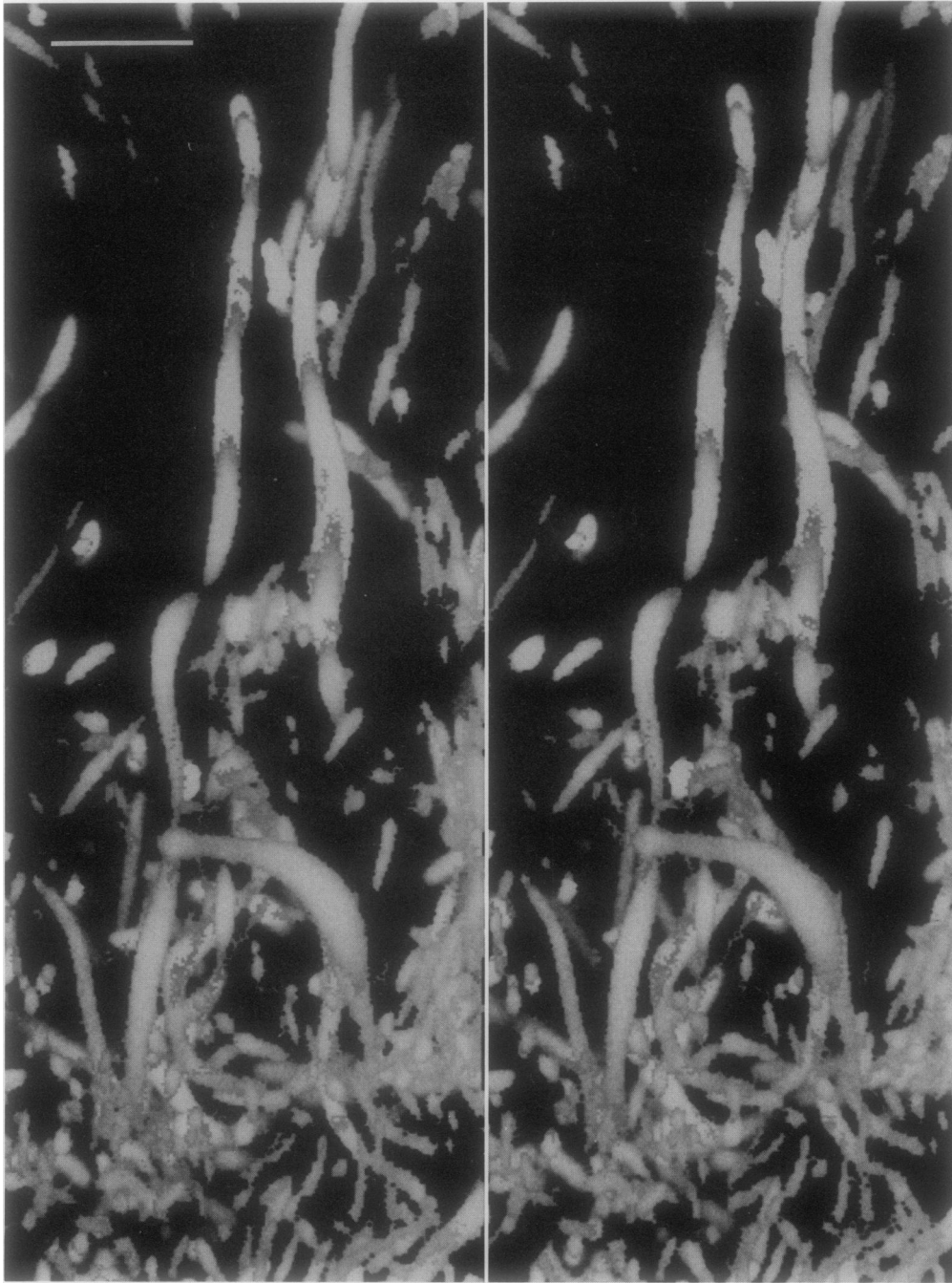


FIG. 6. 3D reconstruction of a *V. parahaemolyticus* biofilm displayed as a stereo pair. The 3D images were obtained by overlaying and aligning seven horizontal optical thin sections taken at 2.0- μm intervals. Bar = 5 μm .

possibly facilitated nutrient flux throughout the biofilm. Channeling and porosity in addition to diffusion processes would explain our observation that the biofilm did not hinder the penetration of the 289-molecular-weight fluorescein molecules into the basal layers of the biofilms studied. This observation supports the findings of Nichols et al. (22) that EPS does not significantly inhibit diffusion of antimicrobial agents. The researchers reported that tobramycin concentrations at the base of a 100- μm -thick biofilm would rise to 90% of the external concentration in only 77 s.

There are a number of technical considerations which must be evaluated before one can fully appreciate the application of confocal laser imaging to the study of microbial biofilms. In addition to being able to section biofilms at a fixed point in time, low-molecular-weight, nontoxic fluorescent compounds (pH, E_h , and cation sensitive, etc.) enable the user to optically probe fully hydrated biofilms at intervals without film disruption. In addition, there are no preparatory steps (such as drying) necessary to facilitate these observations and analyses. These factors will permit

routine time course studies whereby single cells can be monitored until their progeny have ultimately formed a mature biofilm. The effects of induced stresses (inhibitors, antibiotics, and salts, etc.) can thus be evaluated against fully developed biofilms similar to those likely to be targeted in medicine and in industrial control applications. Further, physical parameters of biofilms may be precisely measured by SCLM. Present methods, such as light section microscopy (21), impose inherent limitations on the minimum thickness (8 μm) of the biofilm which may be studied as well as on the precision of the results ($\pm 3 \mu\text{m}$) while offering none of the optical information provided by SCLM (i.e., architecture, cell position, cell number, and amount of noncellular material). The relative ease of SCLM-linked computer 3D reconstruction allows effective visualization of the biofilm in a publishable form. Sagittal sectioning of biofilms also provides a unique side view (xz axis) of cells within the biofilm and of their association with the substratum.

The studies described in this paper confirm the potential for noninvasive imaging of viable biofilms with SCLM by demonstrating the increased resolution and the elimination of defocused haze. In addition, quantitative visualizations of 2D (both xy and xz), 3D, and potentially 4D (time course) reconstructions of biofilm characteristics are possible. When combined with the use of fluorescence probes, SCLM should allow quantitative imaging, mapping, and display in 3D of a broad range of biofilm parameters. Thus, studies utilizing SCLM, particularly in conjunction with other light and electron microscopy techniques, will improve the state of understanding of the structures and natures of both pure- and mixed-species biofilms and will facilitate applied efforts which utilize or involve biofilms in industrial and medical settings.

ACKNOWLEDGMENTS

Byron Zanyk is acknowledged for technical assistance.

The U.S. Office of Naval Research (contract no. N00014-87-G-0249 to D.E.C.) and the Natural Science and Engineering Research Council (NSERC grant to D.E.C.) are acknowledged for financial support.

REFERENCES

- Agard, D. A., Y. Hiraoka, P. Shaw, and J. W. Sedat. 1989. Fluorescence microscopy in three dimensions. *Methods Cell Biol.* **30**:353-377.
- Belas, M. R., and R. R. Colwell. 1982. Adsorption kinetics of laterally and polarly flagellated *Vibrio*. *J. Bacteriol.* **151**:1568-1580.
- Belas, R., M. Simon, and M. Silverman. 1986. Regulation of lateral flagella gene transcription in *Vibrio parahaemolyticus*. *J. Bacteriol.* **167**:210-218.
- Brakenhoff, G. J., H. T. M. van der Voort, M. W. Baarslag, B. Mans, J. L. Oud, R. Zwart, and R. van Driel. 1988. Visualization and analysis techniques for three-dimensional information acquired by confocal microscopy. *Scanning Microsc.* **2**:1831-1838.
- Caldwell, D. E., and J. J. Germida. 1985. Evaluation of difference imagery for visualizing and quantitating microbial growth. *Can. J. Microbiol.* **31**:35-44.
- Caldwell, D. E., D. R. Korber, and J. R. Lawrence. Submitted for publication.
- Caldwell, D. E., and J. R. Lawrence. 1986. Growth kinetics of *Pseudomonas fluorescens* microcolonies within the hydrodynamic boundary layers of surface microenvironments. *Microb. Ecol.* **12**:299-312.
- Caldwell, D. E., and J. R. Lawrence. 1988. Study of attached cells in continuous-flow slide culture, p. 117-138. *In* J. W. T. Wimpenny (ed.), *CRC handbook of laboratory model systems for microbial ecosystems*. CRC Press, Boca Raton, Fla.
- Carlsson, K., and A. Liljeborg. 1989. A confocal laser microscope scanner for digital recording of optical serial sections. *J. Microsc. (Oxford)* **153**:171-180.
- Carlsson, K., P. Wallen, and L. Brodin. 1989. Three-dimensional imaging of neurons by confocal fluorescence microscopy. *J. Microsc. (Oxford)* **155**:15-26.
- Costerton, J. W. 1988. Structure and plasticity at various organization levels in the bacterial cell. *Can. J. Microbiol.* **34**:513-521.
- Costerton, J. W., K.-J. Cheng, G. G. Geesey, T. Ladd, J. C. Nickel, M. Dasgupta, and T. J. Marrie. 1987. Bacterial biofilms in nature and disease. *Annu. Rev. Microbiol.* **41**:435-464.
- Eighmy, T. T., D. Maratea, and P. L. Bishop. 1983. Electron microscopic examination of wastewater biofilm formation and structural components. *Appl. Environ. Microbiol.* **45**:1921-1931.
- Kellogg, S. T. 1989. Three-dimensional ultrastructure of microbial biofilms, abstr. N18. *Abstr. Annu. Meet. Am. Soc. Microbiol.* 1989.
- Kinner, N. E., D. L. Balkwill, and P. L. Bishop. 1983. Light and electron microscopic studies of microorganisms growing in rotating biological contactor biofilms. *Appl. Environ. Microbiol.* **45**:1659-1669.
- Korber, D. R., J. R. Lawrence, B. Sutton, and D. E. Caldwell. 1989. Effect of laminar flow velocity on the kinetics of surface recolonization by Mot^+ and Mot^- *Pseudomonas fluorescens*. *Microb. Ecol.* **18**:1-19.
- Korber, D. R., J. R. Lawrence, L. Zhang, and D. E. Caldwell. 1990. Effect of gravity on bacterial deposition and orientation in laminar flow environments. *Biofouling* **2**:335-350.
- Lawrence, J. R., and D. E. Caldwell. 1987. Behavior of bacterial stream populations within the hydrodynamic boundary layers of surface microenvironments. *Microb. Ecol.* **14**:15-27.
- Lawrence, J. R., P. J. Delaquis, D. R. Korber, and D. E. Caldwell. 1987. Behavior of *Pseudomonas fluorescens* within the hydrodynamic boundary layers of surface microenvironments. *Microb. Ecol.* **14**:1-14.
- Lawrence, J. R., D. R. Korber, and D. E. Caldwell. 1989. Computer enhanced darkfield microscopy for the quantitative analysis of bacterial growth and behavior on surfaces. *J. Microbiol. Methods* **10**:123-138.
- Loeb, G. I. 1980. Measurement of microbial marine fouling films by light section microscopy. *Mar. Technol. Soc. J.* **14**:14-19.
- Nichols, W. W., S. M. Dorrington, M. P. E. Slack, and H. L. Walmsley. 1988. Inhibition of tobramycin diffusion by binding to alginate. *Antimicrob. Agents Chemother.* **32**:518-523.
- Pescod, M. B., and J. V. Nair. 1972. Biological disc filtration for tropical waste treatment. *Experimental studies*. *Water Res.* **6**:1509-1523.
- Robinson, R. W., D. E. Akin, R. A. Nordstedt, M. V. Thomas, and H. C. Aldrich. 1984. Light and electron microscopic examinations of methane-producing biofilms from anaerobic fixed-bed reactors. *Appl. Environ. Microbiol.* **48**:127-136.
- Shotton, D. M. 1989. Confocal scanning optical microscopy and its applications for biological specimens. *J. Cell Sci.* **94**:175-206.
- Shotton, D. M., and N. White. 1989. Confocal scanning microscopy. *Trends Biochem. Sci.* **4**:435-438.
- Wilson, T. 1989. Optical sectioning in confocal fluorescent microscopes. *J. Microsc. (Oxford)* **154**:143-156.
- Woldringh, C. L., M. A. de Jong, W. van den Berg, and L. Koppes. 1977. Morphological analysis of the division cycle of two *Escherichia coli* substrains during slow growth. *J. Bacteriol.* **131**:270-279.